ORIGINAL ARTICLE

Analysis of surface runoff potential in ungauged basin using basin parameters and SCS-CN method

K. Nageswara Rao[1]

Abstract

The present research work was carried out to understand the influence of basin morphometric parameters on runoff potential in an ungauged basin using satellite images, topographical maps, and rainfall data combined with geospatial techniques. The upper Gosthani river basin is an ungauged basin which is located in the Eastern Ghats of Visakhapatnam District, Andhra Pradesh State, Southern India. The river Gosthani and its tributaries are draining through the basin area covering about 321.1 km^2. The quantitative analysis of basin morphometry reveals that the area is under influenced by steep ground slopes, with moderate to less permeable rocks, leading to high runoff. The basin is elongated in shape resulting to flatter peak of flow for longer duration. The daily rainfall data during 2008–2016 were used in the estimation of runoff potential with the help of the Soil Conservation Service-Curve Number (SCS-CN) model. The weighted curve number was determined by the integration of land use and land cover, antecedent moisture condition, and hydrological soil groups. It was observed from the analysis that the overall increase in runoff corresponding to the rainfall. The area receives a good amount of rainfall, but most of it lost as surface runoff (nearly 40% of total rainfall) due to rapid overland flow and impermeable rocks. Analysis of morphometric parameters combined with SCS-CN-based approaches can be explored as an alternative for simulating the hydrological response of the basins.

Keywords Basin morphometry · SCS-CN · Gosthani river basin · Eastern Ghats · Visakhapatnam · Remote sensing and GIS

Introduction

Morphometric characteristics of drainage basin in relation to estimation of surface water potential are utmost importance for planning irrigation, water supply, and flood control projects. Surface or storm runoff is a part of the precipitation which enters the stream immediately after the rainfall. Land use practices, slope, channel gradient, topographical features, and soils can affect the rates and volumes of runoff. Various factors can be human or physical or both control a drainage basin during storm events. Topography is identified as a first-order control on the hydrological response of a basin catchment to rainfall. Understanding the regional hydrology at basin level is very crucial to ascertain the

dynamics of basin. The morphometric analysis of drainage network at a basin scale is being used in describing the process geomorphology, estimation of erosion rates, sediment yields and prediction of flood peaks (Morisawa 1959; Sameena et al. 2009). Runoff response generally depends on the slopes, shapes, lengths, perimeter, and areas of the basin. In the absence of runoff records and other related hydrological information, attempts have been made to relate runoff to the basin geometry using various techniques (Raymond and Anyadike 1989; Maria 2008; Shakil et al. 2012). Mathematical description of the geometry of a drainage basin in terms of measuring linear aspects of channel networks and areal and relief properties of the basin provide basic information to understand various terrain factors like nature of bedrock, infiltration, runoff, and denudation process of the area (Chow 1964; Ward and Robinson 2000). Evaluation by morphometric analysis of a drainage basin and its relevance to hydrological response are well established (Horton 1932, 1945; Strahler 1964; Marathe and Lele 1976; Al-Sulaimi

✉ K. Nageswara Rao
dr.nageswararao@gmail.com

[1] Geography Discipline, School of Sciences, Indira Gandhi National Open University, Maidangarhi, New Delhi 110068, India

1997; Narendra and Nageswara Rao 2006; Somashekar et al. 2011).

Analysing morphological and topographical characteristics of a basin is essential in order to assist in investigating the hydrological response of basins (Zavoinu 1985). The drainage analysis through various morphodynamic variables will help in getting the better conclusions for the assessment of characteristics of stream flow. With the aid of these analyses, the surface runoff would be estimated by considering some physical and environmental variables such as land use and cover, soil and precipitation data using different rainfall-runoff models. The popular model most commonly used for a given rainfall event in an ungauged basin relies on runoff curve numbers developed by the United States Department of Agriculture (USDA) Soil Conservation Service (SCS 1985). This SCS curve number (SCS-CN) model is used for computing the volume of surface runoff in a basin by considering basin characteristics such as soil type, land use/treatment, surface condition, and antecedent moisture condition. The main reason for its wide applicability and acceptability is that it is a simple predictable and stable conceptual method. Chatterjee et al. (1997) used the SCS-CN method in the estimation of surface runoff from small watersheds and found that the predicted runoff hydrographs are in good agreement with the observed runoff hydrographs. Several scientists were tested and analysed this method capabilities, limitations, uses, and its conceptual and empirical validity (Ponce and Hawkins 1996; Moglen 2000; Mishra et al. 2013). Meshram et al. (2017) was calculated CN values by accounting the infiltration and antecedent moisture conditions in Tons River catchment area of India.

Integrated geospatial information technologies for getting the updated information on land use and cover, soil texture, hydrological soil groups, and rainfall data were utilized in runoff potential estimation by applying the SCS-CN method in different regions by various researchers (Melesse and Shih 2002; Jasrotia and Singh 2006; Rolland and Rangarajan 2013). However, most of the studies conducted either analysis of the drainage basins in general or runoff modelling in particular to know the hydrological processes of the areas. Hydrological processes at the basin level can be understood through the measurement of the amount of water entering the area and then the amount that leaves the area of a particular basin. Innovative geospatial information techniques and popular SCS-CN models will provide additional information on hydrological processes that leads to the refinement of the hydrodynamics of the basin.

The present study attempts to analyse the drainage characteristics relate to runoff estimation. In the study area, most of the population are dependent on well and spring water for drinking purposes, whereas water supply for agriculture activities is based on streams and springs source. Most of the streams and springs in the mountainous terrain are either dried up or show reduced discharge from mid-January to the onset of monsoon that leads to water scarcity. However, the area receives noteworthy rainfall, but most of it lost as surface runoff without infiltrating into the surface, due to rapid overland flow on the steep slopes and impermeable rocks. Thus, there is a widespread water shortage in the region. The significant forest alteration is spreading fast in the study area due to various anthropogenic activities, reminding necessity of soil and water conservation to increase the groundwater potential.

Keeping this in view, the present study was conducted with the main objective of runoff estimation and to evaluate drainage characteristics through morphometric analysis in order to understand the hydrological process and predict the hydrological behaviour.

Study area

The study area, Gosthani river basin, is located in the Eastern Ghats of Visakhapatnam District in Andhra Pradesh (AP) state of India. It lies between 18° 08′ 30″ N to 18° 20′ 54″ N latitudes and 82° 56′ 10″ E to 83° 13′ 33″ E longitudes covering about 321.1 km^2 (Fig. 1). The area is characterized by steep mountainous terrain occupied with the hill ranges of Anantagiri and Veduruvada reserved forests of Eastern Ghats. The area experiences tropical humid climate, and temperature recorded is low as 10 °C in January and high as 35 °C in May. The average annual rainfall is 1402 mm contributed mostly from the southwest monsoon between June and September. The region is supported by the total population of 23,379 persons, and out of this 21,578 are scheduled tribe (ST) population accounting to 92.3% (Census 2011). The indigenous tribal groups such as Gadaba, Porja, Khonds, Bhagata, Kotia, and others are accustomed to living in small huts and thatched houses in the dense forest. The economy of the tribes is mainly based on agroforestry, and the majority of the population are having marginal and small land holdings with less than 2 ha. The economy is largely based on a combination of several types of activities. Podu or shifting-type cultivation is commonly practiced by the tribes of this region. Paddy is the predominant crop and is being cultivated by using the terrace method in the valleys and slopes.

Geologically, the area forms a part of the Eastern Ghat Mobile Belt (EGMB) comprising predominantly Khondalites and Charnockites group of rocks of Archaean age and alluvium of Recent age. The bauxitic laterite cappings overlie the Khondalites are exhibiting in brown to red colour. Nearly, 90% of the area is occupied by Khondalite and Charnockite group of rocks. It was recorded that more than 70% of the basin area has the low potential
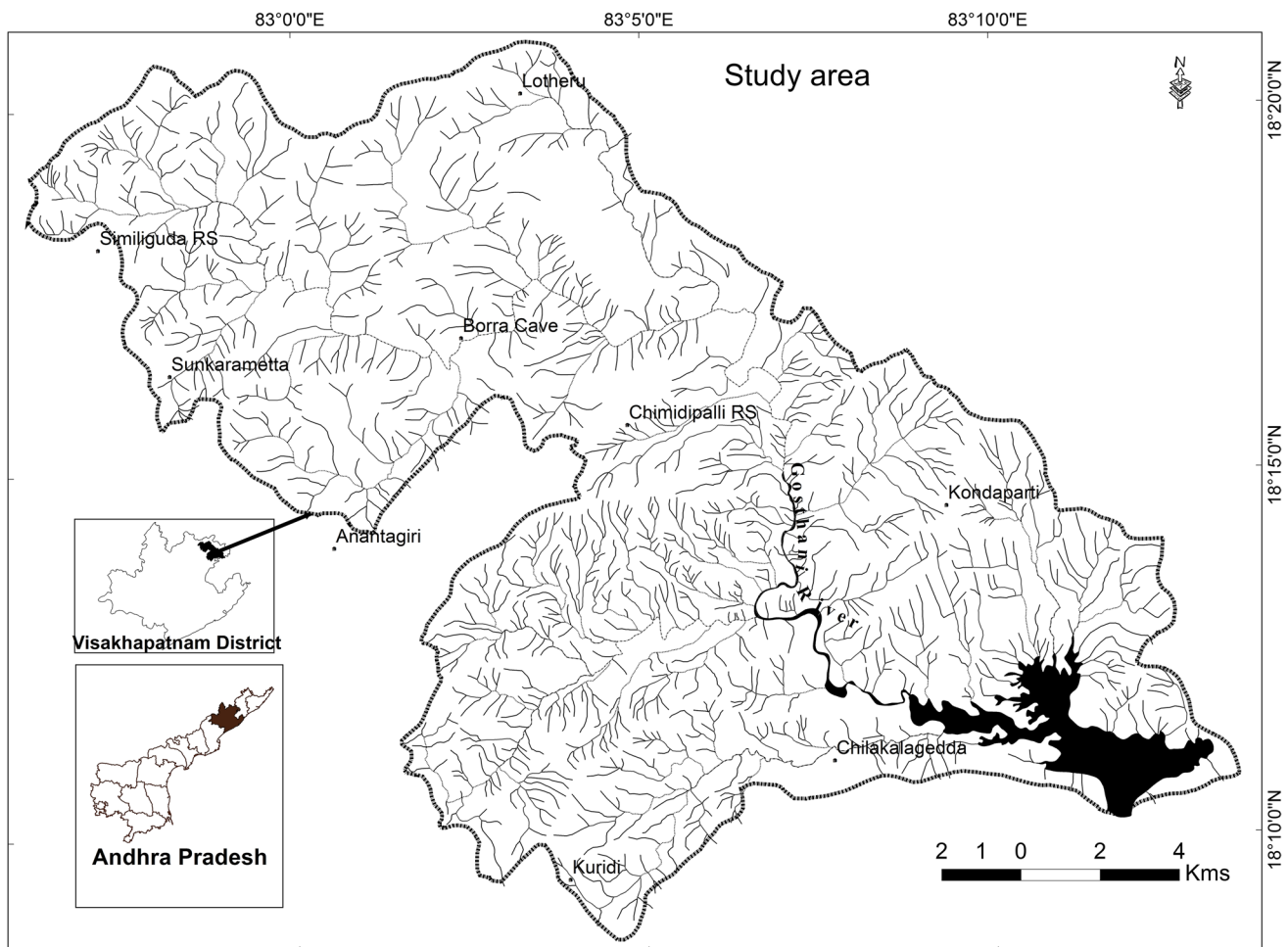
Fig. 1 Location map of the study area depicting drainage network

for groundwater development. The weathered Khondalite material is found with the thickness of about 15–30 m. The quaternary alluvium is made of unconsolidated sediments comprise of boulders, cobbles, pebbles, gravels, sand, silt, and clay, and it is mostly restricted in the valley portions (CGWB 2013). Dug wells and bore wells are well-known abstraction structures that derive groundwater from unconfined to semi-confined aquifers. Both dug well's water and open well's water are utilized for domestic purposes, whereas spring water is mostly used for agriculture needs by the inhabitants of this region. It was observed that some populace is dependent on spring water for domestic use, particularly in summer season due to the scarcity of water. In shallow aquifers, the recorded water levels vary from 2.1 to 8.2 mbgl in pre-monsoon and post-monsoon water levels range from 1.7 to 6.2 mbgl. There is a general fall in groundwater levels in pre-monsoon season and rise in post-monsoon season. In general, the scope of groundwater development is very limited as the area is mostly covered by hard rock terrain.

Materials and methods

In the present study, a different set of data such as toposheets, satellite images, digital elevation model, slope, soil texture map, and rainfall were used for analysing the basin morphometry and runoff. Survey of India toposheets No. 65 N/3, N/4, J/15, and J/16 on 1:50,000 scale were used for the preparation of base map and delineation of upper Gosthani river basin. LISS-IV (IRS-Resourcesat 2) with 5.8 m spatial resolution (2012), and PAN (IRS-P5: Cartosat-1) 2.5 m high spatial resolution (2013) were procured from NRSC, Hyderabad. The area falls in path/rows of 104/60 for LISS-IV and 567 and 568/312 for PAN, respectively. ArcGIS software and ERDAS Imagine software were used for spatial statistical analysis and image processing studies. Geometric rectification of satellite images was carried out by considering road junctions, the intersection of drainage lines, and man-made features of the basemap as ground control points (GCPs). The rectification was performed using the nearest neighbour resampling algorithm with the first-order polynomial transformation and has
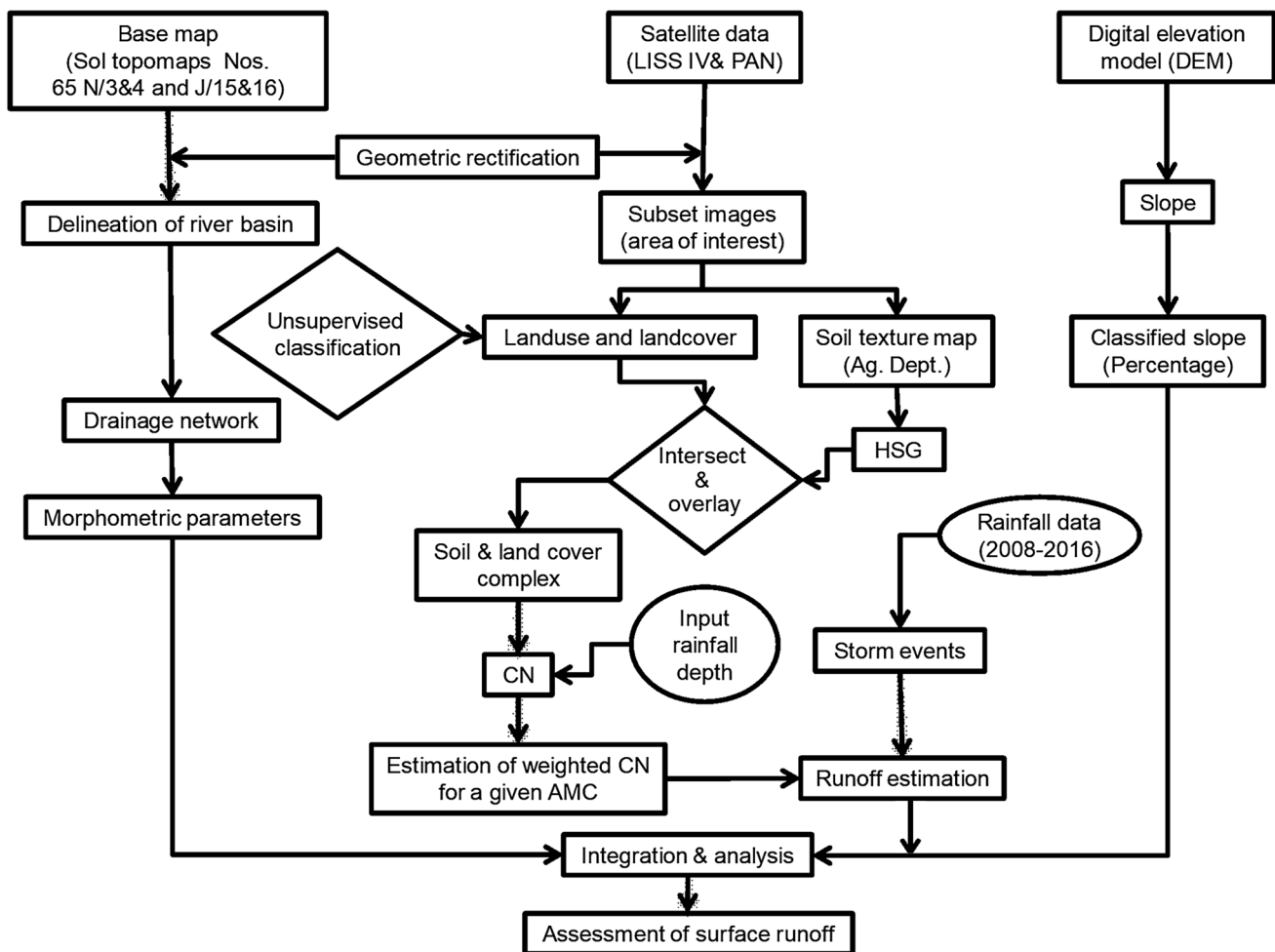
Fig. 2 Flowchart of overall methodology

assigned the projection UTM, WGS-84 datum. False colour composite (FCC) image was interpreted visually to delineate various topographical features based on image characteristics. The drainage network was derived from the base map and updated with the help of satellite data. Edge detection and linear enhancement techniques were applied to extract the drainage layer from the satellite imageries for better interpretation of the stream order. The order was given to each stream by following Strahler (1964) stream ordering technique. ASTER (Advanced Space-borne Thermal Emission and Reflection Radiometer) global digital elevation model (GDEM) data were used to create slope map. GDEM data were obtained from website: http://www.gdem.aster.ersdac.or.jp/ for the purpose of the present research. Land use and land cover analysis was performed using unsupervised classification technique. Soil texture map of the regional State Agricultural Department of Andhra Pradesh was used as a reference in identifying different soil texture classes. The generated soil texture map was then used in the delineation of hydrological soil groups (HSG). The runoff potential was

estimated using various combinations of HSG, land use, and antecedent moisture condition (AMC) classes by following the procedure of the SCS-CN method (SCS 1985). In close proximity to the study area, Indian Meteorological Department (IMD) established one raingauge centre at Anantagiri Mandal Revenue Office of Andhra Pradesh had chosen for collecting daily rainfall data. The data were further analysed for each storm event during the period 2008–2016.

SCS-CN model

The SCS-CN method is based on the water balance equation, and two principle hypotheses are expressed as given below (Mishra and Singh 2003).

$$P = I_a + F + Q \quad \text{(Water balance equation)} \tag{1}$$

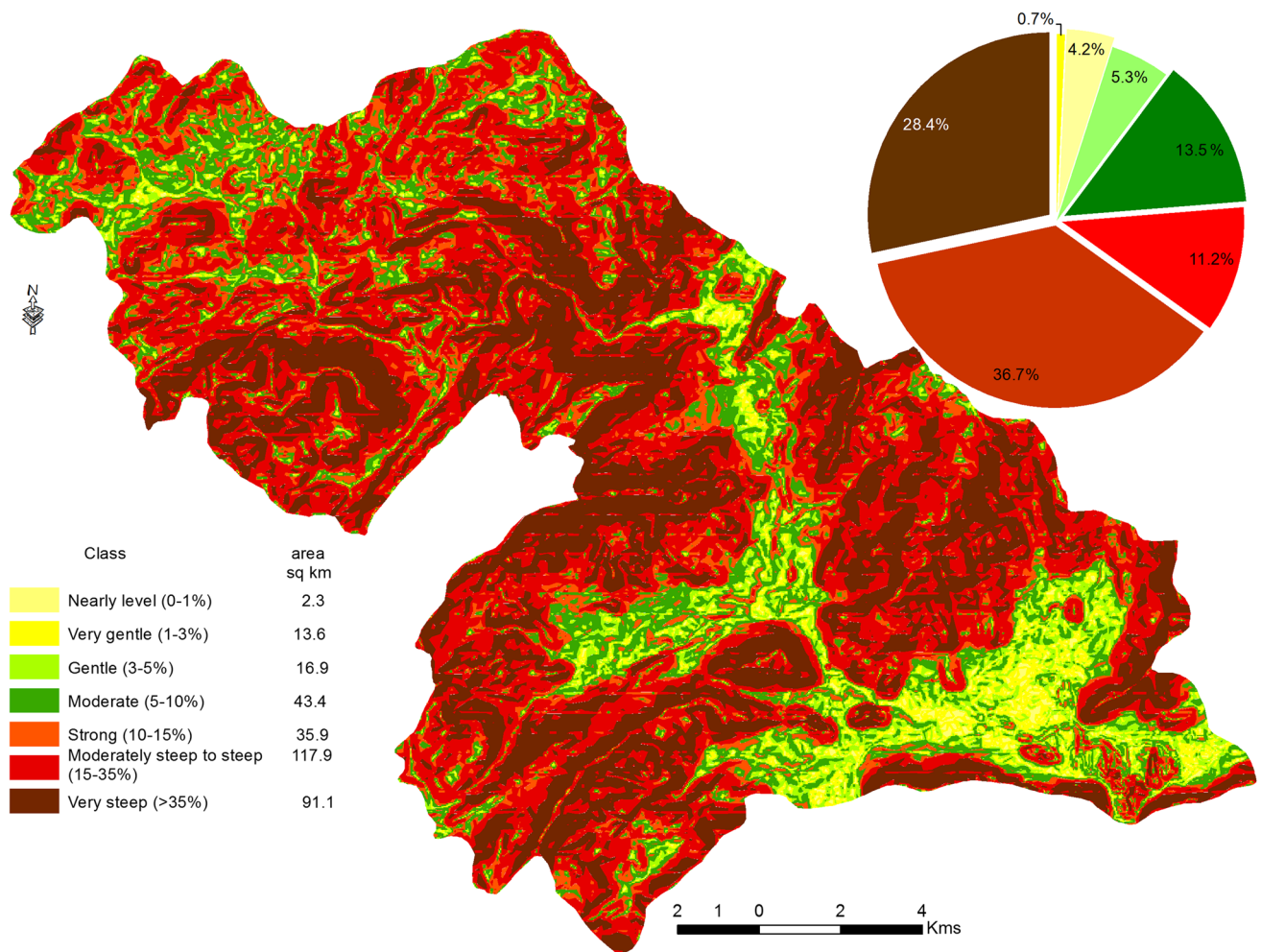$$\frac{Q}{P - I_a} = \frac{F}{S} \quad \text{(Proportional equality hypothesis)} \tag{2}$$

Fig. 3 Distribution of slope categories in percentage of the study area

$I_a = \lambda S$ (Initial abstraction and potential

   maximum retention hypothesis)   (3)

where P is the total precipitation (mm), I_a the initial abstraction (mm), F the cumulative infiltration (mm), Q the direct runoff (mm), S the potential maximum retention or infiltration (mm), and λ the initial abstraction coefficient (0.2) which is dependent on geology and climatic factors.

Mathematically, SCS-CN equation can be expressed as

$$\frac{Q}{P - I_a} = \frac{P - I_a - Q}{S}\qquad(4)$$

This can be rearranged as

$$Q = \frac{\left(P - I_a\right)^2}{\left(P - I_a\right) + S}\ \text{where}\ P > I_a\qquad(5)$$

The initial abstraction I_a is all the losses before runoff begins. It includes the water retained in surface depressions and the water intercepted by vegetation, evaporation, and infiltration. So I_a is highly variable, but generally is correlated with soil and cover parameters. After several studies, I_a was found to be approximated by the following empirical equation.

$$I_a = 0.2S\qquad(6)$$

Substituting I_a in the above Eq. 5, we get

$$Q = \frac{(P - 0.2S)^2}{(P + 0.8S)}\qquad(7)$$

Parameter S varies spatially, due to changes in soils, land use, and slope, and temporally due to changes in soil–water content. In practice, S is derived from a mapping equation expressed in terms of the curve number (CN).

Table 1 Morphometric parameters of upper Gosthani River Basin

Parameter	Symbol	Formula	Value of the basin
Total number of stream orders (Strahler 1964)	$\sum N_u$	Hierarchical rank	1255 (order 1–6)
Cumulative stream length (km) (Horton 1945)	$\sum L_u$	Length of stream	887.2
Bifurcation ratio (Horton 1945)	R_b	N_u/N_{u+1}	4.2 (mean)
Area (km^2)	A		321.1
Perimeter (km)	P		116
Drainage density (km/km^2) (Horton 1945)	D_d	$\sum L_u/A$	2.76
Stream frequency (km/km^2) (Horton 1945)	F_s	$\sum N_u/A$	3.91
Basin length (Horton 1945)	L_b		50.5
Elongation ratio (Schumm 1956)	R_e	$2(A/\pi)^{0.5}/L_b$ $\pi=3.14$ (constant value)	0.4
Circulatory ratio (Miller 1953)	R_c	$4\pi A/P^2$	0.3
Form factor ratio (Horton 1945)	R_f	A/L_b^2	0.13
Length of overland flow (km) (Horton 1945)	L_o	$1/2D_d$	0.18
Constance of channel maintenance (km) (Schumm 1956)	C	$1/D_d$	0.36
Highest elevation (m)	H		1402
Lowest elevation (m)	h		186
Basin relief (m) (Schumm and Hadley 1961)	r	$H–h$	1216
Relative relief (m)	RL_r	$r\times100/P$	1048.3
Time of concentration (Patton 1988)	T_c	$6.95\,(L_b^{1.15}/r^{0.385})$	41.03
Ruggedness number (km) (Schumm 1956)	Rn	$r\times D_d$	3.36

$$S = 25.4\left(\frac{1000}{\text{CN}} - 10\right) \qquad (8)$$

where CN is a dimensionless number varies from 0 to 100. CN is determined from the standard SCS-CN table, based on land use, HSG, and antecedent moisture condition-II. The CN_n is then adjusted for the existing moisture condition. Four groups, namely A, B, C, and D of HSG derived from soil texture classes based on the soil infiltration rate, which is obtained for bare soil after prolonged wetting. AMC is expressed in three categories, viz. I, II, and III, according to rainfall limits for dormant and growing seasons. The weighted curve number was determined for the basin using the following equation.

$$\text{CN}_w = \sum_{i=1}^{n} \frac{\text{CN}_i \times A_i}{A_i} \qquad (9)$$

where CN_i is the curve number for each land use–hydrological soil group, A_i is the area for each land use–hydrological soil group, and n is the class number of land use–hydrological soil group.

Overall methodology of the present study is presented in the form of flowchart in Fig. 2.

Results and discussion

Basin morphometry and runoff

Slope is an important parameter to compute basin geometry towards the assessment of runoff and drainage characteristics. Percentage slope map was generated using DEM. About 76.3% of the basin area falls under strong to very steep slope category (Fig. 3). Thus, the terrain with high slopes of the study area is producing rapid and excessive runoff and increased erosion rate with insignificant recharge potential (IMSD 1995).

Various morphometric parameters such as the linear aspects of the drainage network, areal, and relief aspects of the drainage basin were evaluated with established mathematical equations (Table 1). The first step of drainage analysis is assigning the order to each stream. Stream order (u) is a dimensionless number which can be used for comparison of stream networks on linear scales. The entire basin contains a number of 1255 streams of all orders and is designated as sixth-order basin. The total number of streams of the basin is 976 and 216 for the first order and second order, respectively (Fig. 4). This high proportion indicates that the area is prone to severe erosion. The stream frequency has been decreased as the stream order increases. The analysis of number of streams against stream order on a log-normal
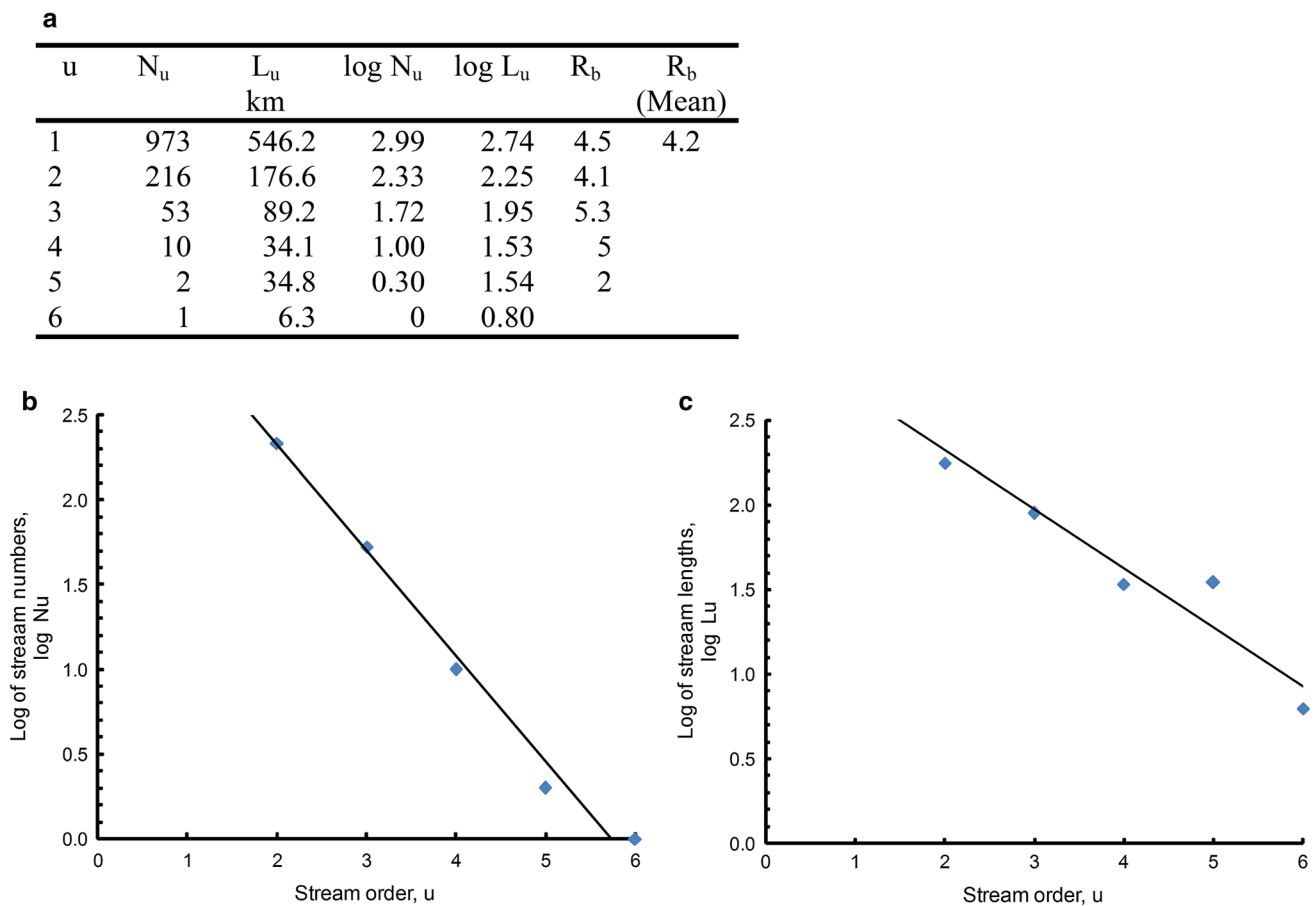
a

u	N_u	L_u km	$\log N_u$	$\log L_u$	R_b	R_b (Mean)
1	973	546.2	2.99	2.74	4.5	4.2
2	216	176.6	2.33	2.25	4.1	
3	53	89.2	1.72	1.95	5.3	
4	10	34.1	1.00	1.53	5	
5	2	34.8	0.30	1.54	2	
6	1	6.3	0	0.80		

Fig. 4 **a** Linear aspects of the drainage network and log-analysis plots, **b** number of streams against stream order, and **c** stream length versus stream order

plot (Fig. 4) shows nearly a straight line which reveals that the number of streams usually decreases in geometric progression as the stream order increases (Horton 1945; Chow 1964). The bifurcation ratio (R_b) ranges between 2 in flat or rolling drainage basins, and 3 to 4 in mountainous or highly dissected drainage basin (Horton 1945). R_b of various orders ranges from 2 to 5.3 with a mean of 4.2 explaining that the basin is highly dissected with a steep gradient leading to less water recharge conditions. Stream length (L_u) explains the hydrological characteristics of the underlying rock strata over the areas of consecutive stream orders. The long length of streams in less number is developed in permeable rocks, while the rock formation is impermeable where the small length of streams formed. High L_u is 546.2 km in the case of first-order streams exhibiting high erosion and low permeability nature of rocks presented in the basin. When the stream order increases, the total length of streams will be decreased (Nageswara Rao et al. 2010). The log-normal plot of stream lengths versus stream order shows the linear pattern with a small deviation (Fig. 4) indicating that

the lithological and topographical variations in the region (Chow 1964).

Areal aspects of a drainage basin control the spatial arrangement, shape and form of drainage systems, and stream discharge and runoff characteristics. The area and perimeter of the Gosthani river basin are about 321.1 km^2 and 116 km, respectively (Table 1). Drainage density (D_d) explains the landscape dissection, infiltration capacity of the land, runoff potential, and the status of vegetative cover (Horton 1932). D_d of the basin is 2.76 km/km^2 indicating that the presence of relatively impermeable subsoil and low groundwater potential. The type of rocks also affects the drainage density. Generally, lower values of D_d tend to occur in granite, gneiss, and schist dominated rocks regions. The major type of rocks in the study area is Khondalites, which falls under the gneissic group of rocks. This condition corroborates the low drainage density which is observed in the basin area. The value of high stream frequency (F_s) exhibits greater surface runoff and steep slopes (Horton 1932, 1945). The computed value of F_s of the basin is 3.91, reflecting that
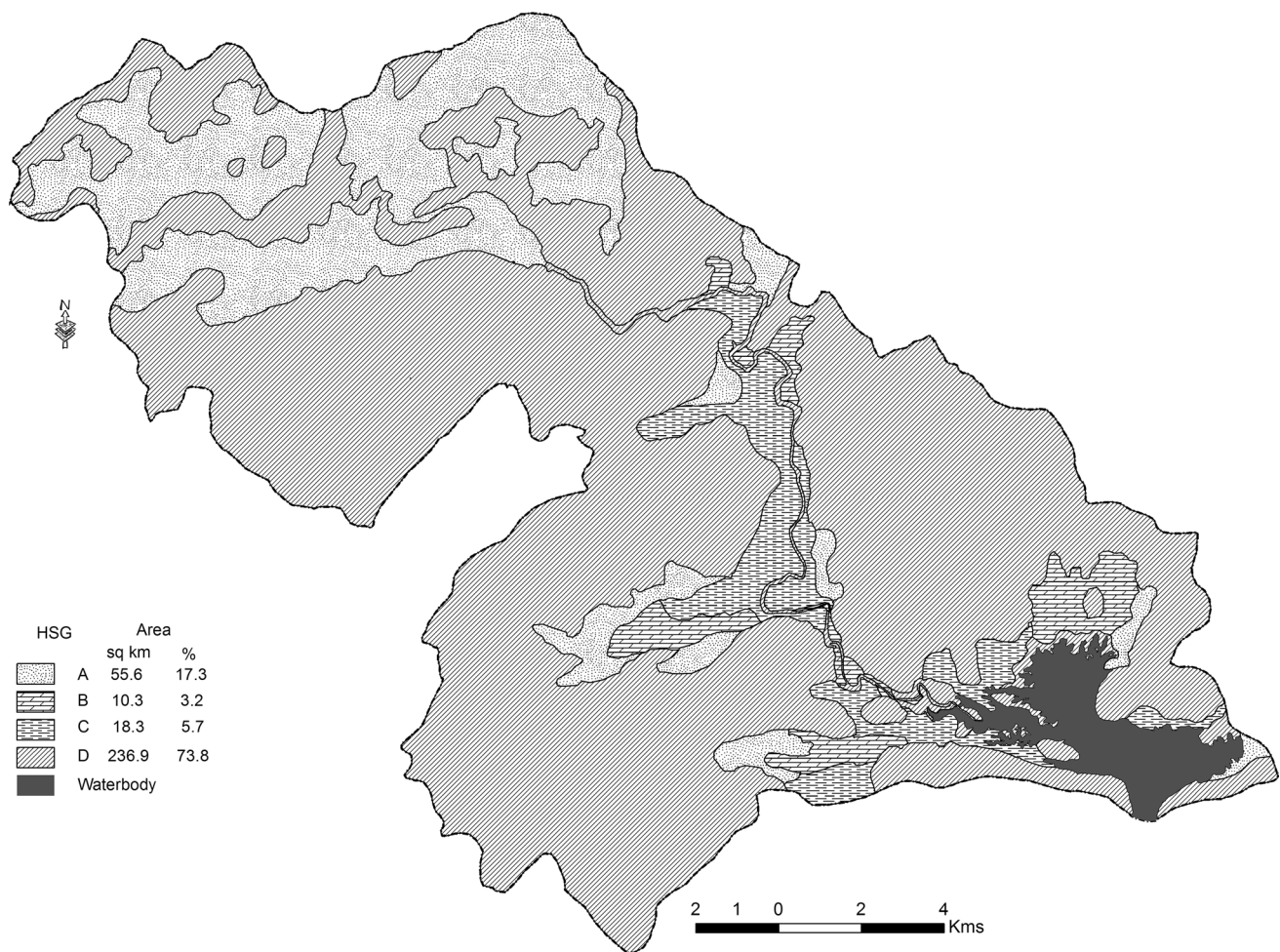
Fig. 5 Hydrological soil groups of the study area

the basin is characterized by high steep slopes and relief, with less permeable rocks that facilitate with high-velocity runoff and less infiltration. Elongation ratio (R_e) of the basin is 0.46 reveals that the basin is elongated in shape and comprising of high-relief and steep slopes (Schumm 1956). Circularity ratio (R_c) is influenced by the length of frequency of stream, geological structure, environmental conditions, relief, and slope of the basin. Low, medium, and high values of R_c explain the young, mature, and old stages of a basin, respectively. If the R_c value is 1.0, the basin is a perfect circle in shape and the discharge quantity would be high (Miller 1953). The R_c value is 0.3 indicating the elongated shape (< 0.5) explains that an early stage of topographical maturity of the basin. Younger stage of tributaries characteristically has high intensity of water flow, which results in the high amount of runoff potential. The form factor ratio (R_f) shows the flow intensity of a basin of the defined area. The R_f varies from 0 (in highly elongated shape) to 1 (in perfect circular shape). The smaller the value of form factor, more elongated will be the basin (Horton 1932). The

R_f value of the basin is 0.13 revealing that elongated basin with the lowest peak flow of longer duration. Constant of channel maintenance (C) is the inverse of drainage density, which generally dependent on the nature and type of rock, environment conditions, relief, and rate of erosion (Schumm 1956). Higher C values have the higher permeability and potential of the area, and vice versa. The low C value (0.36) exhibited in the study area reveals that the area is under the influence of low permeability, very steep slopes, and high runoff potential. The length of overland flow (L_o) explains the length of flow of water over the surface before merges in definite stream channels which affecting both the hydrological and physiographical developments of the drainage basin (Horton 1945). The value of L_o is 0.18 reveals that the basin area has short flow paths, with steep slopes, and more runoff and less infiltration.

Relief aspects of the basin reveal that the topographical gradient characteristics of a basin. The highest elevation, lowest elevation, relief, and relative relief of the basin are 1402 m, 186 m, 1216 m, and 1048.3, respectively. These
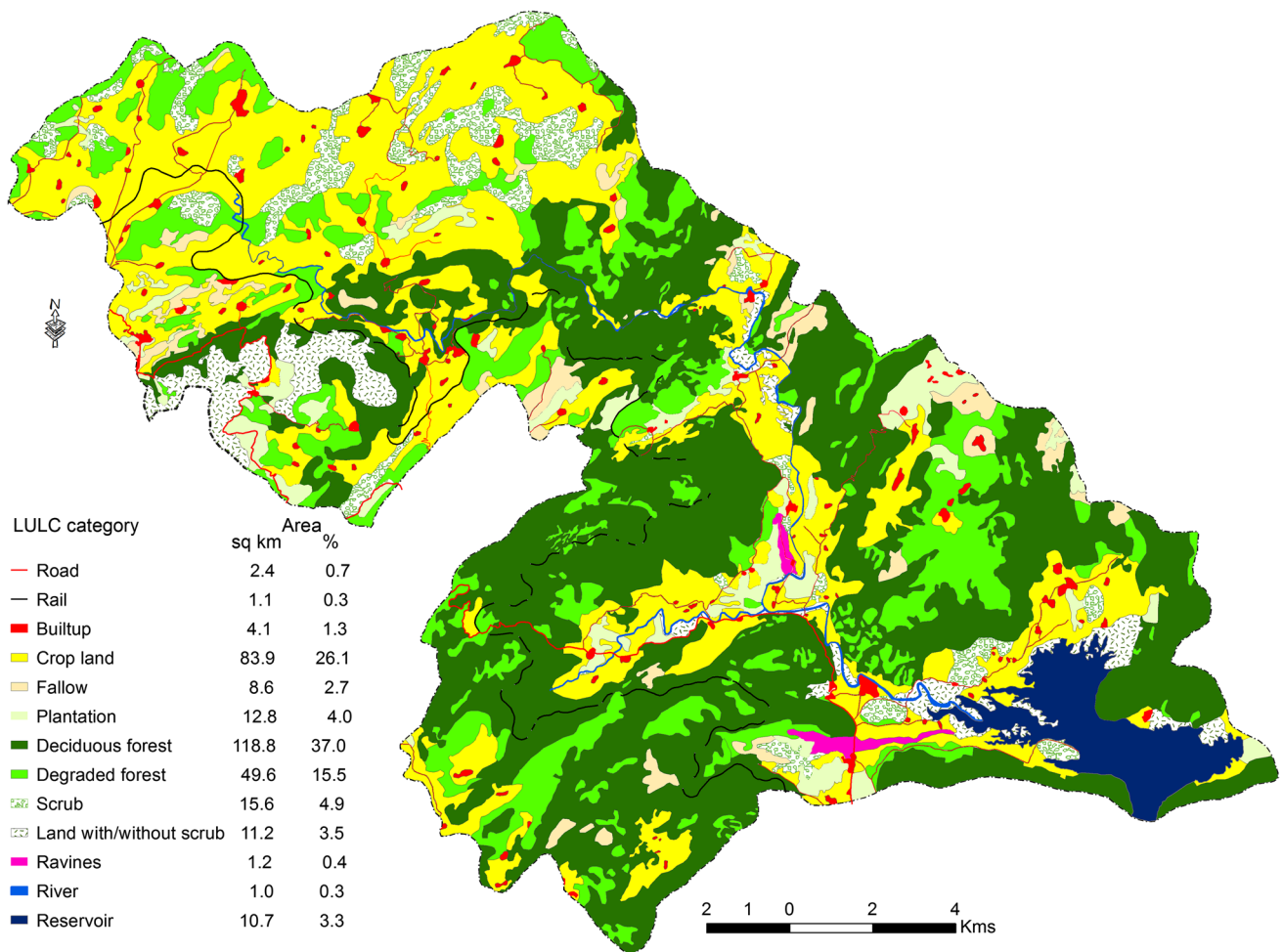
Fig. 6 Land use and land cover features delineated from the satellite data (year 2012)

LULC category	Area sq km	Area %
Road	2.4	0.7
Rail	1.1	0.3
Builtup	4.1	1.3
Crop land	83.9	26.1
Fallow	8.6	2.7
Plantation	12.8	4.0
Deciduous forest	118.8	37.0
Degraded forest	49.6	15.5
Scrub	15.6	4.9
Land with/without scrub	11.2	3.5
Ravines	1.2	0.4
River	1.0	0.3
Reservoir	10.7	3.3

values indicate the presence of less resistant rocks, and also the terrain is on the younger stage of development. The maximum percentage of the area comprises of steep slopes which explain high runoff and low groundwater potential. The Ruggedness number (Rn) is a product of basin relief (*r*) and drainage density (D_d) that indicates the structural complexity of the terrain (Schumm 1956). The Gosthani river basin with a very high Rn value of 3.36 signifies high-relief mountainous terrain. The time of concentration (T_c) is the time taken by water to travel from the most distant point of a basin to its outlet. The high T_c value 41.03 of the basin indicates the highest length of time for water to travel from the most distant point of the basin to its outlet.

All the morphometric parameters of the Gosthani river basin were correlated for each channel network in order to determine their overall effect on runoff potential. Overall, the basin geometry analyses reveal that the network has the greatest influence on surface runoff. Basing on these results, the study was further carried out to estimate the runoff potential by using SCS-CN model.

Runoff estimation through SCS-CN model

Hydrological soil group (HSG)

The soils represented in the study area are brown to red colour. Soil texture can explain the size of soil particles and their arrangement. More than seventy per cent of the area is covered by sandy clay/clay loam type over the thick forest. Soil texture classes were grouped into different hydrological soil groups, namely A, B, C, and D, and their distribution in the study area is presented in Fig. 5. HSG-A consists of sandy loam and loamy sand covers an area of 17.3% of the total area. These soils have low runoff potential. Group-B soils comprising silty loam occupies 3.2% of the area mainly covers the reservoir surroundings. Sandy clay loam soil (HSG-C) covers the central portion of the basin stretches along the river course. HSG-B and -C soils have moderate runoff potential. The group-D which includes sandy clay and clay loam soils cover 73.8% of the total area has very low infiltration and high runoff potential.

Table 2 Distribution of land use with corresponding CN and HSG

Class number (n)	Land use	HSG	CN	Area (A) (km²)	CN×A
1	Built-up	A	77	2.3	175.7
		B	85	0.5	45.3
		C	90	1.3	117.0
		D	92	3.5	322.0
2	Crop land	A	67	41.7	2792.9
		B	78	5.3	414.6
		C	85	9.8	837.1
		D	89	27.1	2407.7
3	Fallow	A	76	1.2	93.3
		B	85	0.6	51.0
		C	90	0.1	8.2
		D	93	6.7	622.7
4	Plantation	A	65	1.6	106.9
		B	73	0.7	49.8
		C	79	2.9	228.5
		D	81	7.5	610.9
5	Forest land	A	25	1.8	45.5
		B	55	0.9	50.6
		C	70	0.8	56.7
		D	77	115.2	8873.7
6	Degraded forest	A	77	3.9	297.6
		B	86	0.2	19.6
		C	91	0.8	72.4
		D	94	44.7	4203.9
7	Scrub	A	68	2.4	160.8
		B	79	0.3	26.0
		C	86	0.9	73.9
		D	89	12.1	1072.9
8	Waste lands	A	68	0.6	39.4
		B	79	1.6	126.1
		C	86	1.8	156.1
		D	89	8.4	751.9

Land use and land cover (LULC)

In the present study, an integrated unsupervised image classification and expert visual interpretation techniques were used to delineate the land use and land cover. In unsupervised classification, a total of forty-five spectral clusters with 95% convergence value were selected to perform the classification for the identification of eight valid classes. The major LULC classes delineated using the unsupervised classification in the study area are built-up, agriculture, forest, wastelands, and water bodies. Field work was carried out rigorously during kharif and rabi seasons for collecting the ground data information of LULC features to ascertain their validity using GPS. The classes were refined into various LULC sub-classes by using expert knowledge coupled with the field data (Fig. 6).

Built-up land in the basin area comprises 2.4% of total area consisting mainly of small hamlets are scattered on slopes and valleys. A very limited extent of the rail and metalled road network are observed in the study area. Most of the hamlets can be reached only by use of cart track or by barefoot, due to inaccessible terrain. Agriculture is the main occupation of the people living in this region, and more than 75% of farmers have very small and marginal holdings of land less than 2 ha. The predominant crop is paddy and also observed rain-fed crops such as jowar, maize, niger, cereals, and pulses in scattered areas. Overall, the agricultural activity is depending mainly on rainfall and the availability of water from rivulets and springs. Plantations like teak, eucalyptus, cashew, mango, coconut, and others are mainly distributed in hilly tracks, slopes, and valley floor regions. In total, the agriculture land forms 32.8% of the total area. Three classes, viz. deciduous forest (37%), degraded forest (15.5%), and scrub (4.9%), are demarcated under forest land. Forest alteration has severely taken place due to overgrazing, and clearance of land for agriculture and built-up purpose. Wastelands are noticed along the river course and the reservoir surroundings. Most of the plateau surfaces contain lateritic cappings and are covered by grass and scrubs. The river Gosthani and its tributaries contribute water to the reservoir are mainly intended to augment water supply to Visakhapatnam urban cluster, and some of it is being utilized for the irrigation purposes in the downstream regions. Except reservoir, no other water bodies are noticed in the basin area.

Integration for estimating surface runoff potential

All the required parameters were integrated for estimating surface water potential according to the adopted methodology. Daily precipitation data are required for the simulation of hydrological processes by the SCS-CN model. In calculating the quantity of runoff from a drainage basin, the curve number is used to determine the amount of excess precipitation that results from a storm event over the basin. Estimation of the curve number requires mapping of HSG and LULC information within the basin boundaries. LULC classes, namely built-up, crop land, fallow, plantation, deciduous forest, degraded forest, scrub, and wastelands, were taken into consideration in order to determine the curve number values. Curve numbers are assigned for each land use–soil group combination of the classes (Table 2). The weighted hydrological curve number is determined for the basin based on antecedent moisture condition (AMC)-II. AMC is the initial moisture condition of the soil, prior to the storm event of interest, and this parameter has taken as an index based

Table 3 Runoff observed for different storm events during 2008–2016

Year	Storm event	Storm rainfall (P) mm	5-day antecedent rainfall mm	AMC class	Runoff (mm)	
					Q	%
2008	February 10–14	101.4	0	I	24.58	24.24
	March 24–25	43.4	0.0	I	1.39	3.21
	May 28–30	29.8	26.2	II	4.13	13.85
	June 2–3	38.5	29.8	II	8.20	21.30
	June 9–12	28.2	118.2	III	11.12	39.45
	July 15–16	38.8	0.0	I	0.68	1.76
	July 20–27	185	38.8	III	157.94	85.37
	July 29–August 12	142.5	24.8	I	50.54	35.46
	August 25–27	58.2	0.0	I	5.09	8.74
	August 29–September 3	237.2	58.2	III	209.51	88.33
	September 8–14	138.4	31.6	II	85.98	62.12
	November 15–18	47.4	0.0	I	2.19	4.62
2009	July 8–16	61.4	23.8	I	6.13	9.98
	July 19–22	31.4	14.4	I	0.05	0.17
	August 30–September 1	80	24	I	13.61	17.01
	September 3–7	47.4	80	III	26.61	56.14
	September 12–14	31.6	1.6	I	0.06	0.20
	September 19–23	73.2	10	I	10.62	14.51
	September 26–27	28.6	58.4	III	11.42	39.92
	October 1–5	158.6	31.8	I	61.95	39.06
	November 12–13	31	7.2	I	0.04	0.13
2010	May 19–23	183.4	0	I	80.51	43.90
	June 7–16	128	0	I	40.79	31.87
	June 28–July 2	44.8	2.4	I	1.65	3.69
	July 4–8	45.3	8.6	I	1.75	3.87
	July 17–31	206.9	0	I	99.00	47.85
	August 11–17	112.8	4.6	I	31.23	27.69
	August 19–31	131	43.6	III	105.04	80.18
	September 3–5	32.6	29	I	0.11	0.34
	September 11–18	287.9	13.8	I	167.20	58.07
	September 29–30	51.2	13.2	I	3.09	6.04
	October 30–November 4	205.2	8.6	I	97.64	47.58
	November 11–14	68.6	0	I	8.76	12.76
	December 6–10	229.2	0	I	117.17	51.12
2011	April 28–29	26.6	5.2	I	0.03	0.10
	May 8–9	52.2	0	I	3.35	6.42
	June 12–15	35.6	1.6	I	0.33	0.92
	July 4–9	91	0	I	18.98	20.86
	July 13–15	56.4	11.8	I	4.53	8.04
	July 25–28	72.6	1.2	I	10.37	14.28
	July 30–August 4	92	72.6	III	67.49	73.36
	August 16–22	102.8	5	I	25.37	24.68
	August 24–28	94.9	37.2	II	48.30	50.90
	August 30–September 2	85	54.4	I	15.97	18.79
	September 11–15	86.6	3.6	I	16.76	19.35
	November 10–12	44.6	0	I	1.62	3.62
	December 31–January 1	60	0	I	5.66	9.44

Table 3 (continued)

Year	Storm event	Storm rainfall (P) mm	5-day antecedent rainfall mm	AMC class	Runoff (mm) Q	%
2012	January 11–12	42	0	I	1.15	2.74
	April 8–12	37	17.8	II	7.43	20.08
	April 16–22	56	67.2	III	34.15	60.99
	April 28–May 1	55	0	I	4.12	7.50
	June 7–10	34	0	I	0.20	0.58
	June 21–22	35.2	0	I	0.29	0.83
	July 12–13	65.4	0	I	7.54	11.54
	July 20–24	52.4	7.8	I	3.40	6.50
	August 2–7	38	3.6	I	0.58	1.53
	August 18–19	17.6	1.4	I	0.91	5.19
	August 26–27	46.4	11.4	I	1.98	4.26
	August 29–September 1	72.2	58	III	48.90	67.72
	September 3–5	30.4	72.2	I	0.02	0.08
	September 9–13	67.4	29	I	8.29	12.31
	September 20–26	45.8	5.4	I	1.85	4.04
	September 28-October 4	119	27.6	I	35.04	29.45
	November 1–7	606.6	0	I	463.46	76.40
2013	April 20–21	30.4	0	I	0.02	0.08
	June 6–9	73.8	26.8	II	31.53	42.72
	June 12–14	48.8	67.4	III	27.82	57.00
	July 22–23	31.6	0	I	0.06	0.20
	August 6–7	48.4	21.2	I	2.41	4.99
	August 15–20	148.4	11.8	I	54.65	36.83
	September 7–13	69.4	0	I	9.07	13.07
	September 16–18	61	33.6	I	6.00	9.83
	October 3–4	68.4	7.2	I	8.68	12.69
	October 7–11	91	68.4	III	66.54	73.12
	October 21–28	320.4	0	I	195.90	61.14
	November 22–23	101.4	0	I	24.58	24.24
2014	May 9–10	40.6	17	III	20.86	51.37
	June 2–5	30.8	0	I	0.03	0.11
	July 9–12	78	42.2	II	34.75	44.55
	July 19–22	41.8	28.4	I	1.12	2.68
	August 20–23	34.8	21.8	I	0.26	0.75
	August 26–31	148.2	22.4	I	54.51	36.78
	September 19–24	78.8	0	I	13.06	16.57
	October 12–13	482.4	0	I	345.15	71.55
	October 17–19	29	482.4	III	11.71	40.38
	December 30–31	48.4	0	I	2.41	4.99

Table 3 (continued)

Year	Storm event	Storm rainfall (P) mm	5-day antecedent rainfall mm	AMC class	Runoff (mm)	
					Q	%
2015	April 16–18	36.8	9.6	I	0.4	1.2
	April 24–25	52.2	0	I	3.4	6.4
	May 12–13	34.8	2.4	I	0.3	0.7
	May 16–17	34.8	54.4	III	16.2	46.4
	June 2–3	64.4	4.2	I	7.2	11.1
	June 5–6	28.8	64.4	III	11.6	40.2
	June 8–9	42.8	76.8	III	22.7	53.0
	June 17–23	180	7.2	I	77.9	43.3
	July 23–24	57	3.4	I	4.7	8.3
	August 9–13	107	0	I	27.8	26.0
	September 9–10	45.2	40.4	II	11.9	26.4
	September 12–17	216.6	75.4	III	189.1	87.3
	September 19–20	43.4	187.4	III	23.2	53.4
	October 15–16	66.8	0	I	8.1	12.1
	November 1–2	32	30.2	I	0.1	0.2
2016	April 1–2	50.4	0	I	2.9	5.7
	May 19–21	140.4	0	I	49.1	35.0
	June 25–July 5	113.2	19.2	II	63.8	56.3
	July 20–26	112.6	11.2	I	31.1	27.6
	July 29–August 7	72	73.8	III	48.7	67.7
	August 25–29	204.6	0	I	97.2	47.5
	September 11–27	425.8	7	I	292.1	68.6
	October 1–3	124.2	0	I	38.3	30.9
	October 5–8	108.2	158.2	III	83.0	76.7

Table 4 Monthly rainfall data (mm) recorded at Anantagiri raingauge centre during 2008–2016. *Source*: IMD raingauge centre, Anantagiri, Visakhapatnam Dt. AP

| Month	Year									Mean
	2008	2009	2010	2011	2012	2013	2014	2015	2016	
January	0.0	0.0	9.4	0.0	90.6	0.0	0.0	38.8	0	15.4
February	101.4	0.0	0.0	12.4	0.0	5.6	0.0	0	0	13.3
March	60.4	46.3	6.8	1.6	10.6	4.2	56.4	8.4	9.4	22.7
April	26.8	26.2	19.8	51.8	215.0	42.2	15.0	98.6	94.8	65.6
May	91.3	20.8	254.8	145.5	32.2	56.8	100.6	107.6	217	114.1
June	196.3	91.0	178.0	66.8	72.0	153.6	44.0	327.4	173.8	144.8
July	284.4	116.6	258.0	266.8	173.1	63.0	189.6	96.4	213	184.5
August	282.7	110.6	270.6	301.3	193.6	244.2	248.4	122	278.2	228.0
September	295.4	213.2	399.9	125.6	173.2	181.4	113.4	357.7	457.2	257.4
October	26.0	152.2	134.6	50.0	104.4	501.0	527.4	139.4	234.6	207.7
November	47.4	63.2	218.0	14.6	606.6	101.4	32.6	56.4	3.2	127.0
December	0.0	0.0	229.2	11.4	0.0	0.0	48.4	2.6	6.2	33.1
Total	1412.1	840.1	1979.1	1047.8	1671.3	1353.4	1375.8	1355.3	1687.4	1413.6
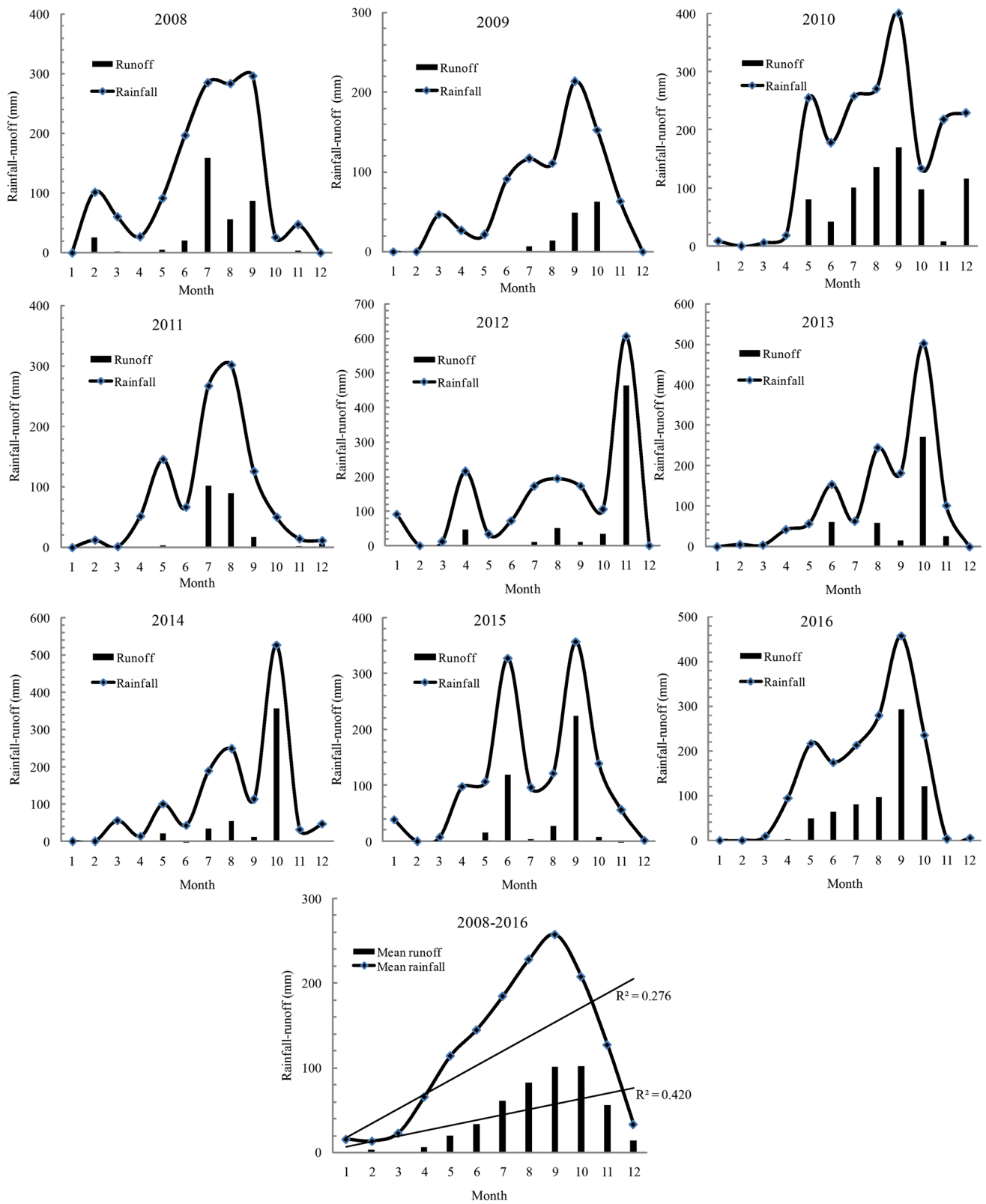
Fig. 7 Rainfall-runoff variations in different months of the period 2008–2016

on seasonal limits of the total 5-day antecedent rainfall. In dormant season, it is less than 12.5 mm, 12.5 to 27.5 mm and more than 27.5 mm for AMC-I, -II, -III, whereas less than 35 mm, 35 to 52.5 mm and more than 52.5 mm in growing season. The calculated weighted CN values are 81 (CN-II), 64 (CN-I), and 91 (CN-III) for corresponding AMC-II, AMC-I, and AMC-III, respectively (Chow 1964). Based on weighted CN values and the rainfall data, the runoff was computed for each storm event. Percentage distribution runoff of each and every storm event during 2008–2016 is given in Table 3. Precipitation is predominantly concentrated during southwest monsoon (June to September) and northeast monsoon (October to November) seasons. Nearly, 55% of annual rainfall is received from SW monsoon, 27% from NE monsoon, and 11% of rainfall as pre-monsoon showers, and December to March are almost rainless months. The average annual rainfall during monsoon (June–November) and non-monsoon (December–May) periods are observed at 1126 mm (82%) and 256 mm (18%), respectively. August is the rainiest month, which is recorded with an average rainfall of 235.9 mm (Table 4). During July to November, the runoff is showing an increasing trend with the rainfall. The insignificant runoff found in the period December to May as rainfall received very less. There is a significant rainfall observed in the month of June, but runoff is very low due to less rainy days. The runoff contribution is generally intensive during the later part of the monsoon month that had been resulted as high observed runoff (Fig. 7). If the storm event rainfall is less than 25 mm, then it was not considered in the runoff determination because it does not have any significant runoff. The majority of storm events were found in the months of September and October. Most of the rainfall occurs during cyclonic storms, which results in peak flows in the streams. Such cyclonic storms are very common during late August, September, October, and November months. During monsoon period, most of the rainwater goes as surface runoff due to the flashy nature of the streams, and the non-monsoon period is almost rainless that leads to the presence of the dry land situation. The average yearly runoff in the basin is estimated to be 454.9 mm which corresponds to 40.6% of average annual rainfall of the basin area.

Conclusion

In the present study, a combined approach of morphometric parameters and SCS-CN methods was used to estimate surface runoff potential in an ungauged basin of the upper Gosthani River basin. The linear, areal, and relief properties of the basin were analysed. The impact of drainage on runoff variations during 2008–2016 was evaluated. The results revealed that the understanding of basin geometry is much essential in runoff estimation. The basin is found to be strongly elongated with a circularity ratio of 0.3 and elongation ratio of 0.46. A circular basin is more efficient in the discharge of runoff than the elongated basin. The low value of drainage intensity (2.76 km/km^2) reveals that the greater surface runoff and steep slopes, and surface are affected by the agents of denudation. The erosional processes of fluvial origin are predominantly influenced by the subsurface lithology of the basin. Runoff in the basin was gradually increasing for the past seven years accounts 33% of total annual precipitation. As the basin underlain by crystalline rocks, the quantity of recharge through springs and other sources is very less during non-monsoon season because the infiltration of rainwater in short spells lasted for a less-time period. Soil texture and forest cover are the dominant factors for increasing upstream runoff that perhaps caused by the heavy precipitation in short spells. Stream runoff in the slopes was influenced by human activities severely, because of slash and burn agricultural methods. The water resource management could make scientific plans for water utilization according to runoff formation and change characteristics in the study area. The suitable groundwater structures, namely check dams, percolation tanks, bench terrace, and contour bunds, may be constructed after detailed studies of groundwater prospective zones.

The morphometric parameters and runoff evaluated using geospatial techniques will help to understand various terrain parameters such as the nature of the bedrock, infiltration capacity, and surface condition and also watershed prioritization for soil and water conservation at a microlevel. In conclusion, the methodology used in this study may be limited to measuring the quantity of runoff potential, but it would be helpful where the runoff records were not available.

Compliance with ethical standards

References

Al-Sulaimi J, Khalaf F, Mukhopadhyay A (1997) Geomorphological analysis of paleo drainage systems and their environmental implications in the desert of Kuwait. Environ Geol 29(1/2):94–11

Census (2011) Census statistics. Govt. of India, New Delhi

CGWB (2013) Ground water brochure, Visakhapatnam District, Andhra Pradesh. Central Ground Water Board, Ministry of Water Resources, Government of India

Chatterjee C, Jha R, Lohani AK, Jaiswal RK (1997) Determination of SCS curve number and land use changes for Hamidnagar sub-basin of Punpun basin. CS (AR) 14/96-97, National Institute of Hydrology, Roorkee

Chow VT (1964) Handbook of applied hydrology. McGraw Hill, New York

Horton RE (1932) Drainage basin characteristics. Trans Am Geophys Union 13:350–361

Horton RE (1945) Erosional development of streams and their drainage basins: hydrophysical approach to quantitative morphology. Bull Geol Soc Am 56:275–370

IMSD (1995) Integrated mission for sustainable development technical guidelines. National Remote Sensing Agency, Department of Space, Govt. of India, pp 1–127

Jasrotia AS, Singh R (2006) Modeling runoff and soil erosion in a catchment area using the GIS in the Himalayan region, India. Environ Geol 51:29–37

Marathe AR, Lele VS (1976) Quantitative geomorphology of the drainage basins of Bhadar and Hiran rivers, Saurashtra, Western India. Bull Deccan Coll Res Inst 36(1–4):97–109

Maria YEA (2008) Morphometric analysis of Colanguil river basin and flash flood hazard, San Juan, Argentina. Environ Geol 55:107–111

Melesse AM, Shih SF (2002) Spatially distributed storm runoff depth estimation using Landsat images and GIS. Comp Electr Agri 37(1–3):173–183

Meshram SG, Sharma SK, Tignath S (2017) Application of remote sensing and geographical information system for generation of runoff curve number. Appl Water Sci 7:1773–1779. https://doi.org/10.1007/s13201-015-0350-7

Miller VC (1953) A quantitative geomorphic study of drainage basin characteristics in the Clinch Mountain area, Varginia and Tennessee. Project NR 389-042, Technical Report 3, Columbia University, Department of Geology, ONR, Geography Branch, New York

Mishra SK, Singh VP (2003) Soil conservation service curve number (SCS-CN) methodology. Kluwer Academic Publishers, Dordrecht

Mishra SK, Gajbhiye S, Pandey A (2013) Estimation of design runoff curve numbers for Narmada watersheds (India). J Appl Water Eng Res 1(1):69–79

Moglen GE (2000) Effect of orientation of spatially distributed curve numbers in runoff calculations. J Am Water Res Assoc 36(6):1391–1400

Morisawa ME (1959) Relation of morphometric properties to runoff in the Little Mill Creek, Ohio, drainage basin. Technical report 17, Columbia University Department of Geology, ONR, New York

Nageswara Rao K, Narendra K, Swarna Latha P (2010) An integrated study of geospatial information technologies for surface runoff estimation in an agricultural watershed, India. J Indian Soc Remote Sens 38:255–267

Narendra K, Nageswara Rao K (2006) Morphometry of the Mehadrigedda watershed, Visakhapatnam District, Andhra Pradesh using GIS and Resourcesat data. J Indian Soc Remote Sens 34(2):101–110

Patton P (1988) Drainage basin morphometry and floods. In: Baker V, Kochel R, Patton P (eds) Flood geomorphology. Wiley, New York, pp 51–65

Ponce VM, Hawkins RH (1996) Runoff curve number: has it reached maturity? J Hydrol Eng 1(1):11–19

Raymond NC, Anyadike Phillip OP (1989) Runoff response to basin parameters in south eastern Nigeria. Phys Geogr 71(1/2):75–84

Rolland A, Rangarajan R (2013) Runoff estimation and potential recharge site delineation using analytic hierarchy process. Geocarto Int 28:159–170

Sameena M, Krishnamurthy J, Jayaraman V, Ranganna G (2009) Evaluation of drainage networks developed in hard rock terrain. Geocarto Int 24(5):397–420

Schumm SA (1956) Evaluation of drainage systems and slopes in badlands at Perth Amboy, New Jersy. Geol Soc Am Bull 67(5):597–646

Schumm SA, Hadley RF (1961) Progress in the application of landform analysis in studies of semiarid erosion: Geol Surv Cir 437. USGS, Washington

SCS (1985) National engineering handbook, section 4-hydrology, United States Department of Agriculture Soil Conservation Service, Washington D.C

Shakil AR, Shakeel AB, Irfan R (2012) Geoinformatics for assessing the morphometric control hydrological response at watershed scale in the upper Indus basin. J Earth Syst Sci 121(3):659–686

Somashekar RK, Ravikumar P, Sowmya SV, Mubhashir AD, Ravikumar AS (2011) Runoff estimation and morphometric analysis for Hesaraghatta watershed using IRS–1D LISS III FCC satellite data. J Indian Soc Remote Sens 39(1):95–106

Strahler AN (1964) Quantitative geomorphology of drainage basins and channel networks. In: Chow VT (ed) Handbook of applied hydrology, section 4-II. McGraw Hill Book Company, New York, pp 39–76

Ward RC, Robinson M (2000) Principles of hydrology. McGraw-Hill, Maidenhead

Zavoinu I (1985) Morphometry of drainage basins. Elsevier, Amsterdam